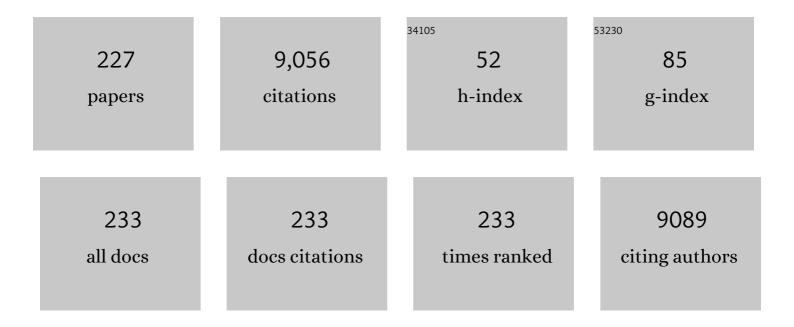
List of Publications by Year in descending order

Source: https://exaly.com/author-pdf/9038668/publications.pdf Version: 2024-02-01



RUNAVELL

#	Article	IF	CITATIONS
1	Self-powered stretchable strain sensors for motion monitoring and wireless control. Nano Energy, 2022, 92, 106754.	16.0	27
2	Cooperative control of perpendicular magnetic anisotropy via crystal structure and orientation in freestanding SrRuO3 membranes. Npj Flexible Electronics, 2022, 6, .	10.7	21
3	Isostructural metal-insulator transition driven by dimensional-crossover in <mml:math xmlns:mml="http://www.w3.org/1998/Math/MathML"> <mml:msub> <mml:mi>SrIrO </mml:mi> <mml:mn> 3 heterostructures. Physical Review Materials, 2022, 6, .</mml:mn></mml:msub></mml:math 	ıl:m₂n≄ <td>ml:ænsub></td>	ml :æ nsub>
4	Emergence of Insulating Ferrimagnetism and Perpendicular Magnetic Anisotropy in 3d–5d Perovskite Oxide Composite Films for Insulator Spintronics. ACS Applied Materials & Interfaces, 2022, 14, 15407-15414.	8.0	8
5	Liquid Metal Based Nano-Composites for Printable Stretchable Electronics. Sensors, 2022, 22, 2516.	3.8	11
6	An Antifatigue Liquid Metal Composite Electrode Ionic Polymer-Metal Composite Artificial Muscle with Excellent Electromechanical Properties. ACS Applied Materials & Interfaces, 2022, 14, 14630-14639.	8.0	17
7	Ultraâ€robust stretchable electrode for eâ€skin: In situ assembly using a nanofiber scaffold and liquid metal to mimic waterâ€toâ€net interaction. InformaÄnÃ-Materiály, 2022, 4, .	17.3	47
8	0D/1D/2D architectural Co@C/MXene composite for boosting microwave attenuation performance in 2–18ÂGHz. Carbon, 2022, 193, 182-194.	10.3	108
9	A flexible dual-gate hetero-synaptic transistor for spatiotemporal information processing. Nanoscale Advances, 2022, 4, 2412-2419.	4.6	13
10	Thickness-dependent and strain-tunable magnetism in two-dimensional van der Waals VSe2. Nano Research, 2022, 15, 7597-7603.	10.4	19
11	Effects of Si content on structure and soft magnetic properties of Fe81.3SixB17-xCu1.7 nanocrystalline alloys with pre-existing α-Fe nanocrystals. Journal of Materials Science, 2021, 56, 2539-2548.	3.7	11
12	Stretchable and Twistable Resistive Switching Memory with Information Storage and Computing Functionalities. Advanced Materials Technologies, 2021, 6, 2000810.	5.8	10
13	A visible light-triggered artificial photonic nociceptor with adaptive tunability of threshold. Nanoscale, 2021, 13, 1029-1037.	5.6	9
14	Electric Field Control of Magnetic Properties by Means of Li+ Migration in FeRh Thin Film. Magnetochemistry, 2021, 7, 45.	2.4	1
15	Mechanical Analysis and Experimental Studies of the Transverse Strain in Wrinkled Metallic Thin Films. Metals, 2021, 11, 427.	2.3	1
16	Bioâ€Inspired Multiâ€Mode Painâ€Perceptual System (MMPPS) with Noxious Stimuli Warning, Damage Localization, and Enhanced Damage Protection. Advanced Science, 2021, 8, 2004208.	11.2	17
17	Phase Manipulating toward Molybdenum Disulfide for Optimizing Electromagnetic Wave Absorbing in Gigahertz. Advanced Functional Materials, 2021, 31, 2011229.	14.9	141
18	Hydrogen Bonding in Self-Healing Elastomers. ACS Omega, 2021, 6, 9319-9333.	3.5	79

#	Article	IF	CITATIONS
19	A flexible metamaterial based on liquid metal patterns embedded in magnetic medium for lightweight microwave absorber. Materials Research Bulletin, 2021, 137, 111199.	5.2	8
20	Liquid Metalâ€Based Strain Sensor with Ultralow Detection Limit for Human–Machine Interface Applications. Advanced Intelligent Systems, 2021, 3, 2000235.	6.1	33
21	Multiâ€Mode Painâ€Perceptual System: Bioâ€Inspired Multiâ€Mode Painâ€Perceptual System (MMPPS) with Noxious Stimuli Warning, Damage Localization, and Enhanced Damage Protection (Adv. Sci. 10/2021). Advanced Science, 2021, 8, 2170055.	11.2	1
22	Effect of isothermal crystallization in antiferromagnetic IrMn on the formation of spontaneous exchange bias. Applied Physics Letters, 2021, 118, .	3.3	7
23	Lateral Modulation of Magnetic Anisotropy in Tricolor 3d–5d Oxide Superlattices. ACS Applied Electronic Materials, 2021, 3, 4210-4217.	4.3	5
24	Dumbbell-Like Fe ₃ O ₄ @N-Doped Carbon@2H/1T-MoS ₂ with Tailored Magnetic and Dielectric Loss for Efficient Microwave Absorbing. ACS Applied Materials & Interfaces, 2021, 13, 47061-47071.	8.0	62
25	Liquid Metalâ€Based Strain Sensor with Ultralow Detection Limit for Human–Machine Interface Applications. Advanced Intelligent Systems, 2021, 3, 2170073.	6.1	7
26	Crystal Orientations Dependent Polarization Reversal in Ferroelectric PbZr 0.2 Ti 0.8 O 3 Thin Films for Multilevel Data Storage Applications. Advanced Materials Interfaces, 2021, 8, 2100871.	3.7	3
27	Colossal angular magnetoresistance in the antiferromagnetic semiconductor <mml:math xmlns:mml="http://www.w3.org/1998/Math/MathML"><mml:msub><mml:mi>EuTe</mml:mi><mml:mn>2Physical Review B, 2021, 104, .</mml:mn></mml:msub></mml:math 	l:m_{ືສ.2i}	ml: n æub>
28	Controllable and Stable Quantized Conductance States in a Pt/HfO <i>_x</i> /ITO Memristor. Advanced Electronic Materials, 2020, 6, 1901055.	5.1	31
29	A Stretchable Capacitive Strain Sensor Having Adjustable Elastic Modulus Capability for Wideâ€Range Force Detection. Advanced Engineering Materials, 2020, 22, 1901239.	3.5	12
30	Manipulation of Exchange Bias Effect via All-Solid-State <mml:math xmlns:mml="http://www.w3.org/1998/Math/MathML" display="inline" overflow="scroll"><mml:mi>Li</mml:mi> -Ion Redox Capacitor with Antiferromagnetic Electrode. Physical Review Applied, 2020, 14, .</mml:math 	3.8	16
31	Magnetism modulation and conductance quantization in a gadolinium oxide memristor. Physical Chemistry Chemical Physics, 2020, 22, 26322-26329.	2.8	6
32	Magnetocrystalline anisotropy imprinting of an antiferromagnet on an amorphous ferromagnet in FeRh/CoFeB heterostructures. NPG Asia Materials, 2020, 12, .	7.9	18
33	Emergent Ferroelectricity in Otherwise Nonferroelectric Oxides by Oxygen Vacancy Design at Heterointerfaces. ACS Applied Materials & Interfaces, 2020, 12, 45602-45610.	8.0	15
34	Anti-oxidative passivation and electrochemical activation of black phosphorus <i>via</i> covalent functionalization and its nonvolatile memory application. Journal of Materials Chemistry C, 2020, 8, 7309-7313.	5.5	11
35	Synthesis of single-crystal La0.67Sr0.33MnO3 freestanding films with different crystal-orientation. APL Materials, 2020, 8, .	5.1	31
36	A Stretchable Capacitive Strain Sensor Having Adjustable Elastic Modulus Capability for Wideâ€Range Force Detection. Advanced Engineering Materials, 2020, 22, 2070011.	3.5	6

#	Article	IF	CITATIONS
37	Inferring the magnetic anisotropy of a nanosample through dynamic cantilever magnetometry measurements. Applied Physics Letters, 2020, 116, 193102.	3.3	4
38	Layer-by-layer epitaxial growth of monoclinic SrIrO3 thin films on (111)-oriented SrTiO3 through interface engineering. Thin Solid Films, 2020, 709, 138119.	1.8	2
39	Materials with strong spin-textured bands. Npj Quantum Materials, 2020, 5, .	5.2	13
40	Preparation and magnetic properties of wrinkled FeRh flexible films. AIP Advances, 2020, 10, 025327.	1.3	3
41	A Wearable Capacitive Sensor Based on Ring/Diskâ€Shaped Electrode and Porous Dielectric for Noncontact Healthcare Monitoring. Global Challenges, 2020, 4, 1900079.	3.6	29
42	Strain-Insensitive Elastic Surface Electromyographic (sEMG) Electrode for Efficient Recognition of Exercise Intensities. Micromachines, 2020, 11, 239.	2.9	8
43	Waterproof, Highly Tough, and Fast Self-Healing Polyurethane for Durable Electronic Skin. ACS Applied Materials & Interfaces, 2020, 12, 11072-11083.	8.0	149
44	Piezocapacitive Flexible E‣kin Pressure Sensors Having Magnetically Grown Microstructures. Advanced Materials Technologies, 2020, 5, 1900934.	5.8	78
45	Emergent ferromagnetism with tunable perpendicular magnetic anisotropy in short-periodic SrIrO3/SrRuO3 superlattices. Applied Physics Letters, 2020, 116, .	3.3	13
46	Stress-coefficient of magnetoelastic anisotropy in flexible Fe, Co and Ni thin films. Journal of Magnetism and Magnetic Materials, 2020, 505, 166750.	2.3	8
47	Ultrathin MoS ₂ Nanosheets Encapsulated in Hollow Carbon Spheres: A Case of a Dielectric Absorber with Optimized Impedance for Efficient Microwave Absorption. ACS Applied Materials & Interfaces, 2020, 12, 20785-20796.	8.0	120
48	Oxygen vacancy enhanced ferroelectricity in BTO:SRO nanocomposite films. Acta Materialia, 2020, 199, 9-18.	7.9	12
49	Stretchable tactile sensor with high sensitivity and dynamic stability based on vertically aligned urchin-shaped nanoparticles. Materials Today Physics, 2020, 14, 100219.	6.0	20
50	A univariate ternary logic and three-valued multiplier implemented in a nano-columnar crystalline zinc oxide memristor. RSC Advances, 2019, 9, 24595-24602.	3.6	6
51	Quantum Conductance: Recent Advances of Quantum Conductance in Memristors (Adv. Electron.) Tj ETQq1 1	0.784314 5.1	rgBT /Overloc
52	Asymmetric Structure Based Flexible Strain Sensor for Simultaneous Detection of Various Human Joint Motions. ACS Applied Electronic Materials, 2019, 1, 1866-1872.	4.3	35
53	Implementation of All 27 Possible Univariate Ternary Logics With a Single ZnO Memristor. IEEE Transactions on Electron Devices, 2019, 66, 4710-4715.	3.0	15
54	Recent Advances of Quantum Conductance in Memristors. Advanced Electronic Materials, 2019, 5, 1800854.	5.1	44

#	Article	IF	CITATIONS
55	Magnetic softness and magnetization dynamics of FeSiBNbCu(P,Mo) nanocrystalline alloys with good high-frequency characterization. Journal of Magnetism and Magnetic Materials, 2019, 478, 192-197.	2.3	29
56	Reversibly controlled magnetic domains of Co film via electric field driven oxygen migration at nanoscale. Applied Physics Letters, 2019, 114, .	3.3	11
57	Method for Assembling Nanosamples and a Cantilever for Dynamic Cantilever Magnetometry. Physical Review Applied, 2019, 11, .	3.8	9
58	Controlled Construction of Atomic Point Contact with 16 Quantized Conductance States in Oxide Resistive Switching Memory. ACS Applied Electronic Materials, 2019, 1, 789-798.	4.3	25
59	The evolution of relaxation modes during isothermal annealing and its influence on properties of Fe-based metallic glass. Journal of Non-Crystalline Solids, 2019, 509, 95-98.	3.1	18
60	An Oxide Schottky Junction Artificial Optoelectronic Synapse. ACS Nano, 2019, 13, 2634-2642.	14.6	237
61	Redox gated polymer memristive processing memory unit. Nature Communications, 2019, 10, 736.	12.8	99
62	Thin and broadband Ce2Fe17N3-Î′/MWCNTs composite absorber with efficient microwave absorption. Journal of Alloys and Compounds, 2019, 787, 1097-1103.	5.5	20
63	xmlns:mml="http://www.w3.org/1998/Math/MathML" display="inline" overflow="scroll"> <mml:msub><mml:mi>Co</mml:mi><mml:mn>40</mml:mn></mml:msub> <ml mathvariant="normal">B<mml:mn>20</mml:mn>Thin Films via All-Solid-State <mml:math displ.<="" td="" xmlns:mml="http://www.w3.org/1998/Math/MathML"><td>nl:mj>Fehath></td><td>mm<mark>l:</mark>mi><mn 11</mn </td></mml:math></ml 	nl:mj>Fehath>	mm <mark>l:</mark> mi> <mn 11</mn
64	Physical Review Applied, 2019, 12, . Magnetoelastic anisotropy of antiferromagnetic materials. Applied Physics Letters, 2019, 115, .	3.3	12
65	Nanoscale magnetization reversal by electric field-induced ion migration. MRS Communications, 2019, 9, 14-26.	1.8	7
66	Flexible supercapacitor electrodes fabricated by dealloying nanocrystallized Al-Ni-Co-Y-Cu metallic glasses. Journal of Alloys and Compounds, 2019, 772, 164-172.	5.5	26
67	Printable Liquidâ€Metal@PDMS Stretchable Heater with High Stretchability and Dynamic Stability for Wearable Thermotherapy. Advanced Materials Technologies, 2019, 4, 1800435.	5.8	92
68	Intrinsically Stretchable Resistive Switching Memory Enabled by Combining a Liquid Metal–Based Soft Electrode and a Metal–Organic Framework Insulator. Advanced Electronic Materials, 2019, 5, 1800655.	5.1	53
69	Ten States of Nonvolatile Memory through Engineering Ferromagnetic Remanent Magnetization. Advanced Functional Materials, 2019, 29, 1806460.	14.9	15
70	Organic and hybrid resistive switching materials and devices. Chemical Society Reviews, 2019, 48, 1531-1565.	38.1	291
71	Direct imaging of cross-sectional magnetization reversal in an exchange-biased CoFeB/IrMn bilayer. Physical Review B, 2018, 97, .	3.2	11
72	Improving Unipolar Resistive Switching Uniformity with Cone-Shaped Conducting Filaments and Its Logic-In-Memory Application. ACS Applied Materials & Interfaces, 2018, 10, 6453-6462.	8.0	68

#	Article	IF	CITATIONS
73	Lattice-Mismatch-Induced Oscillatory Feature Size and Its Impact on the Physical Limitation of Grain Size. Physical Review Applied, 2018, 9, .	3.8	9
74	Amorphous microwires of high entropy alloys with large magnetocaloric effect. Intermetallics, 2018, 96, 79-83.	3.9	48
75	Polyaniline-poly(vinylidene fluoride) blend microfiltration membrane and its spontaneous gold recovery application. Science China Chemistry, 2018, 61, 118-126.	8.2	4
76	Electromagnetic and microwave-absorbing properties of Co-based amorphous wire and Ce2Fe17N3-δ composite. Journal of Alloys and Compounds, 2018, 730, 255-260.	5.5	32
77	Enhanced and broadband absorber with surface pattern design for X-Band. Current Applied Physics, 2018, 18, 55-60.	2.4	8
78	Industrialization of a FeSiBNbCu nanocrystalline alloy with high Bs of 1.39ÂT and outstanding soft magnetic properties. Journal of Materials Science: Materials in Electronics, 2018, 29, 19517-19523.	2.2	11
79	Mechano-regulated metal–organic framework nanofilm for ultrasensitive and anti-jamming strain sensing. Nature Communications, 2018, 9, 3813.	12.8	57
80	Elastic Conductors: A Composite Elastic Conductor with High Dynamic Stability Based on 3D-Calabash Bunch Conductive Network Structure for Wearable Devices (Adv. Electron. Mater. 9/2018). Advanced Electronic Materials, 2018, 4, 1870045.	5.1	0
81	A novel approach based on magneto-electric torque sensor for non-contact biomarkers detection. Sensors and Actuators B: Chemical, 2018, 276, 540-544.	7.8	4
82	Spin-valve-like magnetoresistance in a Ni-Mn-In thin film. Physical Review B, 2018, 97, .	3.2	4
83	A Composite Elastic Conductor with High Dynamic Stability Based on 3Dâ€Calabash Bunch Conductive Network Structure for Wearable Devices. Advanced Electronic Materials, 2018, 4, 1800137.	5.1	57
84	2D Magnetic Mesocrystals for Bit Patterned Media. Advanced Materials Interfaces, 2018, 5, 1800997.	3.7	12
85	Recyclable Liquid Metalâ€Based Circuit on Paper. Advanced Materials Technologies, 2018, 3, 1800131.	5.8	32
86	Anomalous Hall magnetoresistance in a ferromagnet. Nature Communications, 2018, 9, 2255.	12.8	39
87	A skin-inspired tactile sensor for smart prosthetics. Science Robotics, 2018, 3, .	17.6	195
88	Fast decolorization of azo dyes in both alkaline and acidic solutions by Al-based metallic glasses. Journal of Alloys and Compounds, 2017, 701, 759-767.	5.5	92
89	Nanoporous metal/metal-oxide composite prepared by one-step de-alloying AlNiCoYCu metallic glasses. Journal of Alloys and Compounds, 2017, 703, 461-465.	5.5	21
90	Microwave absorbing properties of FeCrMoNiPBCSi amorphous powders composite. Journal of Alloys and Compounds, 2017, 705, 309-313.	5.5	27

#	Article	IF	CITATIONS
91	Highly flexible resistive switching memory based on amorphous-nanocrystalline hafnium oxide films. Nanoscale, 2017, 9, 7037-7046.	5.6	109
92	Rapid detection of Escherichia coli O157:H7 using tunneling magnetoresistance biosensor. AIP Advances, 2017, 7, .	1.3	21
93	Effect of epitaxial strain and lattice mismatch on magnetic and transport behaviors in metamagnetic FeRh thin films. AIP Advances, 2017, 7, .	1.3	24
94	Enhanced stress-invariance of magnetization direction in magnetic thin films. Applied Physics Letters, 2017, 111, .	3.3	22
95	Determination of stress-coefficient of magnetoelastic anisotropy in flexible amorphous CoFeB film by anisotropic magnetoresistance. Applied Physics Letters, 2017, 111, .	3.3	19
96	Light-Gated Memristor with Integrated Logic and Memory Functions. ACS Nano, 2017, 11, 11298-11305.	14.6	173
97	Nanochannels: A 1D Vanadium Dioxide Nanochannel Constructed via Electricâ€Fieldâ€Induced Ion Transport and its Superior Metal–Insulator Transition (Adv. Mater. 39/2017). Advanced Materials, 2017, 29, .	21.0	1
98	High-throughput investigation of orientations effect on nanoscale magnetization reversal in cobalt ferrite thin films induced by electric field. Applied Physics Letters, 2017, 111, 162401.	3.3	9
99	A 1D Vanadium Dioxide Nanochannel Constructed via Electricâ€Fieldâ€Induced Ion Transport and its Superior Metal–Insulator Transition. Advanced Materials, 2017, 29, 1702162.	21.0	79
100	Recovery of gold from hydrometallurgical leaching solution of electronic waste via spontaneous reduction by polyaniline. Progress in Natural Science: Materials International, 2017, 27, 514-519.	4.4	33
101	Magnetic anisotropy and high-frequency property of flexible FeCoTa films obliquely deposited on a wrinkled topography. Scientific Reports, 2017, 7, 2837.	3.3	23
102	Fe78Si9B13 amorphous powder core with improved magnetic properties. Journal of Materials Science: Materials in Electronics, 2017, 28, 1180-1185.	2.2	7
103	Microwave absorption properties of planar-anisotropy Ce 2 Fe 17 N 3 â^î^r powders/Silicone composite in X-band. Journal of Magnetism and Magnetic Materials, 2017, 424, 39-43.	2.3	28
104	Nonlinear fragile-to-strong transition in a magnetic glass system driven by magnetic field. AIP Advances, 2017, 7, 125014.	1.3	2
105	Functional Oxide Thin Films and Nanostructures: Growth, Interface, and Applications. Journal of Nanomaterials, 2016, 2016, 1-2.	2.7	1
106	Organic Biomimicking Memristor for Information Storage and Processing Applications. Advanced Electronic Materials, 2016, 2, 1500298.	5.1	181
107	Magnetostrictive GMR spin valves with composite FeGa/FeCo free layers. AIP Advances, 2016, 6, .	1.3	22
108	Effect of IrMn inserted layer on anomalous-Hall resistance and spin-Hall magnetoresistance in Pt/IrMn/YIG heterostructures. Journal of Applied Physics, 2016, 120, .	2.5	6

#	Article	IF	CITATIONS
109	Tuning magnetic anisotropy of amorphous CoFeB film by depositing on convex flexible substrates. AIP Advances, 2016, 6, .	1.3	21
110	Surface morphology and magnetic property of wrinkled FeGa thin films fabricated on elastic polydimethylsiloxane. Applied Physics Letters, 2016, 108, .	3.3	26
111	Stretchable Spin Valve with Stable Magnetic Field Sensitivity by Ribbon-Patterned Periodic Wrinkles. ACS Nano, 2016, 10, 4403-4409.	14.6	57
112	Synaptic plasticity and learning behaviours in flexible artificial synapse based on polymer/viologen system. Journal of Materials Chemistry C, 2016, 4, 3217-3223.	5.5	61
113	In Situ Nanoscale Electric Field Control of Magnetism by Nanoionics. Advanced Materials, 2016, 28, 7658-7665.	21.0	52
114	Fieldlike spin-orbit torque in ultrathin polycrystalline FeMn films. Physical Review B, 2016, 93, .	3.2	31
115	Reversible Luminescence Modulation upon an Electric Field on a Full Solid-State Device Based on Lanthanide Dimers. ACS Applied Materials & Interfaces, 2016, 8, 15551-15556.	8.0	8
116	Flexural Strength and Weibull Analysis of Bulk Metallic Glasses. Journal of Materials Science and Technology, 2016, 32, 129-133.	10.7	19
117	Interactions of Shear Bands in a Ductile Metallic Glass. Journal of Iron and Steel Research International, 2016, 23, 48-52.	2.8	11
118	Dynamic magnetic characteristics of Fe78Si13B9 amorphous alloy subjected to operating temperature. Journal of Magnetism and Magnetic Materials, 2016, 408, 159-163.	2.3	13
119	Influence of Thermal Deformation on Exchange Bias in FeGa/IrMn Bilayers Grown on Flexible Polyvinylidene Fluoride Membranes. IEEE Transactions on Magnetics, 2016, 52, 1-4.	2.1	4
120	Convertible resistive switching characteristics between memory switching and threshold switching in a single ferritin-based memristor. Chemical Communications, 2016, 52, 4828-4831.	4.1	71
121	An organic terpyridyl-iron polymer based memristor for synaptic plasticity and learning behavior simulation. RSC Advances, 2016, 6, 25179-25184.	3.6	48
122	Fabrication of FeSiBPNb amorphous powder cores with high DC-bias and excellent soft magnetic properties. Journal of Magnetism and Magnetic Materials, 2016, 401, 432-435.	2.3	48
123	Development of FeNiNbSiBP bulk metallic glassy alloys with excellent magnetic properties and high glass forming ability evaluated by different criterions. Intermetallics, 2016, 71, 1-6.	3.9	19
124	Correlation between soft-magnetic properties and Tx1-Tc in high Bs FeCoSiBPC amorphous alloys. Journal of Alloys and Compounds, 2016, 659, 193-197.	5.5	72
125	Switching Memory: An Optoelectronic Resistive Switching Memory with Integrated Demodulating and Arithmetic Functions (Adv. Mater. 17/2015). Advanced Materials, 2015, 27, 2812-2812.	21.0	0
126	Anisotropic field-induced melting of orbital ordered structure inPr0.6Ca0.4MnO3. Physical Review B, 2015, 91, .	3.2	7

#	Article	IF	CITATIONS
127	Magnetization reversal in epitaxial exchange-biased IrMn/FeGa bilayers with anisotropy geometries controlled by oblique deposition. Physical Review B, 2015, 91, .	3.2	19
128	Extraordinary Hall resistance and unconventional magnetoresistance in <mml:math xmlns:mml="http://www.w3.org/1998/Math/MathML"><mml:msub><mml:mrow><mml:mi>Pt</mml:mi><mml:m Physical Review B, 2015, 92, .</mml:m </mml:mrow></mml:msub></mml:math 	lox∦.2∥mml	:m b ≱ <mml:m< td=""></mml:m<>
129	Pure spin-Hall magnetoresistance in Rh/Y3Fe5O12 hybrid. Scientific Reports, 2015, 5, 17734.	3.3	25
130	Strain assisted electrocaloric effect in PbZr0.95Ti0.05O3 films on 0.7Pb(Mg1/3Nb2/3)O3-0.3PbTiO3 substrate. Scientific Reports, 2015, 5, 16164.	3.3	9
131	Magnetocaloric effect of Fe–RE–B–Nb (RE = Tb, Ho or Tm) bulk metallic glasses with high glass-forming ability. Journal of Alloys and Compounds, 2015, 644, 346-349.	5.5	16
132	An Optoelectronic Resistive Switching Memory with Integrated Demodulating and Arithmetic Functions. Advanced Materials, 2015, 27, 2797-2803.	21.0	174
133	Static and high frequency magnetic properties of FeGa thin films deposited on convex flexible substrates. Applied Physics Letters, 2015, 106, .	3.3	52
134	Nonvolatile Memory: Metalâ€Organic Framework Nanofilm for Mechanically Flexible Information Storage Applications (Adv. Funct. Mater. 18/2015). Advanced Functional Materials, 2015, 25, 2630-2630.	14.9	1
135	Modulation of Magnetic Anisotropy in Flexible Multiferroic FeGa/PVDF Heterostructures Under Various Strains. IEEE Transactions on Magnetics, 2015, 51, 1-4.	2.1	1
136	Preparation of nanoporous silver micro-particles through ultrasonic-assisted dealloying of Mg-Ag alloy ribbons. Materials Letters, 2015, 144, 138-141.	2.6	8
137	Fe-based amorphous alloys for wide ribbon production with high Bs and outstanding amorphous forming ability. Journal of Alloys and Compounds, 2015, 630, 209-213.	5.5	106
138	Thermally assisted electric field control of magnetism in flexible multiferroic heterostructures. Scientific Reports, 2015, 4, 6925.	3.3	12
139	Role of the Co-based microwires/polymer matrix interface on giant magneto impedance response. Journal of Alloys and Compounds, 2015, 643, S95-S98.	5.5	2
140	Magnetoinductance and magnetoimpedance response of Co-based multi-wire arrays. Journal of Magnetism and Magnetic Materials, 2015, 393, 278-283.	2.3	5
141	Fabrication of FePBNbCr Glassy Cores With Good Soft Magnetic Properties by Hot Pressing. IEEE Transactions on Magnetics, 2015, 51, 1-4.	2.1	3
142	Push–Pull Type Oligo(<i>N</i> -annulated perylene)quinodimethanes: Chain Length and Solvent-Dependent Ground States and Physical Properties. Journal of the American Chemical Society, 2015, 137, 8572-8583.	13.7	93
143	Metalâ€Organic Framework Nanofilm for Mechanically Flexible Information Storage Applications. Advanced Functional Materials, 2015, 25, 2677-2685.	14.9	133
144	2D Nanovaristors at Grain Boundaries Account for Memristive Switching in Polycrystalline BiFeO ₃ . Advanced Electronic Materials, 2015, 1, 1500019.	5.1	11

#	Article	IF	CITATIONS
145	Nanoscale Magnetization Reversal Caused by Electric Field-Induced Ion Migration and Redistribution in Cobalt Ferrite Thin Films. ACS Nano, 2015, 9, 4210-4218.	14.6	60
146	Magnetocaloric effect in Fe–Tm–B–Nb metallic glasses near room temperature. Journal of Non-Crystalline Solids, 2015, 425, 114-117.	3.1	27
147	Magnetic Anisotropy and Reversal in Epitaxial FeGa/MgO(001) Films Deposited at Oblique Incidence. IEEE Transactions on Magnetics, 2015, 51, 1-4.	2.1	2
148	Preparation and magnetic properties of (Co0.6Fe0.3Ni0.1)70â^'x (B0.811Si0.189)25+x Nb5 bulk glassy alloys. Journal of Materials Science: Materials in Electronics, 2015, 26, 7006-7012.	2.2	7
149	Evolution of shear bands into cracks in metallic glasses. Journal of Alloys and Compounds, 2015, 621, 238-243.	5.5	22
150	Synthesis and nonvolatile memristive switching effect of a donor–acceptor structured oligomer. Journal of Materials Chemistry C, 2015, 3, 664-673.	5.5	29
151	The magnetocaloric effect of Gd-Tb-Dy-Al-M (MÂ=ÂFe, Co and Ni) high-entropy bulk metallic glasses. Intermetallics, 2015, 58, 31-35.	3.9	84
152	Crystallization Behavior of FeSiBPCu Nanocrystalline Soft-Magnetic Alloys with High Fe Content. Science of Advanced Materials, 2015, 7, 2721-2725.	0.7	12
153	Unusual anisotropic magnetoresistance in charge-orbital ordered Nd0.5Sr0.5MnO3 polycrystals. Journal of Applied Physics, 2014, 116, .	2.5	4
154	Electric-field control of magnetic anisotropy in Fe81Ga19/BaTiO3 heterostructure films. AIP Advances, 2014, 4, 117113.	1.3	14
155	Tunneling magnetoresistance induced by controllable formation of Co filaments in resistive switching Co/ZnO/Fe structures. Europhysics Letters, 2014, 108, 58004.	2.0	20
156	Transparent Electronics: Thermally Stable Transparent Resistive Random Access Memory based on Allâ€Oxide Heterostructures (Adv. Funct. Mater. 15/2014). Advanced Functional Materials, 2014, 24, 2110-2110.	14.9	2
157	A Resistance-Switchable and Ferroelectric Metal–Organic Framework. Journal of the American Chemical Society, 2014, 136, 17477-17483.	13.7	103
158	Resistance-Switchable Graphene Oxide-Polymer Nanocomposites for Molecular Electronics. ChemElectroChem, 2014, 1, 514-519.	3.4	21
159	Anomalous anisotropic magnetoresistance effects in graphene. AIP Advances, 2014, 4, 097101.	1.3	6
160	Magneto-mechanical coupling effect in amorphous Co40Fe40B20 films grown on flexible substrates. Applied Physics Letters, 2014, 105, .	3.3	60
161	Thermally Stable Transparent Resistive Random Access Memory based on Allâ€Oxide Heterostructures. Advanced Functional Materials, 2014, 24, 2171-2179.	14.9	150
162	Intrinsic and interfacial effect of electrode metals on the resistive switching behaviors of zinc oxide films. Nanotechnology, 2014, 25, 425204.	2.6	49

#	Article	IF	CITATIONS
163	Thermally-stable resistive switching with a large ON/OFF ratio achieved in poly(triphenylamine). Chemical Communications, 2014, 50, 11856-11858.	4.1	69
164	Structural effect on the resistive switching behavior of triphenylamine-based poly(azomethine)s. Chemical Communications, 2014, 50, 11496-11499.	4.1	42
165	<i>para</i> â€Quinodimethaneâ€Bridged Perylene Dimers and Pericondensed Quaterrylenes: The Effect of the Fusion Mode on the Ground States and Physical Properties. Chemistry - A European Journal, 2014, 20, 11410-11420.	3.3	46
166	Ion transport-related resistive switching in film sandwich structures. Science Bulletin, 2014, 59, 2363-2382.	1.7	9
167	High strength CoFe-based glassy alloy with high thermal stability. Materials Letters, 2014, 114, 126-128.	2.6	6
168	Polymer memristor for information storage and neuromorphic applications. Materials Horizons, 2014, 1, 489.	12.2	209
169	Composition Effect on Intrinsic Plasticity or Brittleness in Metallic Glasses. Scientific Reports, 2014, 4, 5733.	3.3	23
170	Positive temperature coefficient of magnetic anisotropy in polyvinylidene fluoride (PVDF)-based magnetic composites. Scientific Reports, 2014, 4, 6615.	3.3	34
171	Anisotropic magnetoresistance in epitaxial La0.67(Ca1â^'xSrx)0.33MnO3 films. Journal of Applied Physics, 2013, 113, 17C722.	2.5	7
172	Controllable strain-induced uniaxial anisotropy of Fe81Ga19 films deposited on flexible bowed-substrates. Journal of Applied Physics, 2013, 114, .	2.5	39
173	Dibenzoheptazethrene Isomers with Different Biradical Characters: An Exercise of Clar's Aromatic Sextet Rule in Singlet Biradicaloids. Journal of the American Chemical Society, 2013, 135, 18229-18236.	13.7	167
174	Role of oxadiazole moiety in different D–A polyazothines and related resistive switching properties. Journal of Materials Chemistry C, 2013, 1, 4556.	5.5	56
175	Magnetic field induced polarization and magnetoelectric effect of Ba0.8Ca0.2TiO3-Ni0.2Cu0.3Zn0.5Fe2O4 nanomultiferroic. Journal of Applied Physics, 2013, 113, .	2.5	37
176	Pushing Extended <i>p</i> -Quinodimethanes to the Limit: Stable Tetracyano-oligo(<i>N</i> -annulated) Tj ETQq0 () 0 rgBT /(13.7	Overlock 10 170
177	Effect of buffer layer and external stress on magnetic properties of flexible FeGa films. Journal of Applied Physics, 2013, 113, .	2.5	33
178	In-plane anisotropic converse magnetoelectric coupling effect in FeGa/polyvinylidene fluoride heterostructure films. Journal of Applied Physics, 2013, 113, .	2.5	17
179	Strain induced tunable anisotropic magnetoresistance in La0.67Ca0.33MnO3/BaTiO3 heterostructures. Journal of Applied Physics, 2013, 113, 17C716.	2.5	9
180	Preparation and ferroelectric properties of freestanding Pb(Zr,Ti)O ₃ thin membranes. Journal Physics D: Applied Physics, 2012, 45, 185302.	2.8	21

#	Article	IF	CITATIONS
181	Mechanically tunable magnetic properties of Fe81Ga19 films grown on flexible substrates. Applied Physics Letters, 2012, 100, .	3.3	93
182	Mechanism for resistive switching in an oxide-based electrochemical metallization memory. Applied Physics Letters, 2012, 100, .	3.3	117
183	Tunable photovoltaic effects in transparent Pb(Zr0.53,Ti0.47)O3 capacitors. Applied Physics Letters, 2012, 100, .	3.3	58
184	Nonvolatile bistable resistive switching in a new polyimide bearing 9-phenyl-9H-carbazole pendant. Journal of Materials Chemistry, 2012, 22, 520-526.	6.7	70
185	A Multilevel Memory Based on Proton-Doped Polyazomethine with an Excellent Uniformity in Resistive Switching. Journal of the American Chemical Society, 2012, 134, 17408-17411.	13.7	136
186	Resistive switching effects in oxide sandwiched structures. Frontiers of Materials Science, 2012, 6, 183-206.	2.2	68
187	Anisotropic magnetoresistance in polycrystalline La _{0.67} (Ca _{1â^'x} Sr _x) _{0.33} MnO ₃ . Journal Physics D: Applied Physics, 2012, 45, 245001.	2.8	17
188	Observation of Conductance Quantization in Oxideâ€Based Resistive Switching Memory. Advanced Materials, 2012, 24, 3941-3946.	21.0	217
189	Resistive Switching Memories: Observation of Conductance Quantization in Oxideâ€Based Resistive Switching Memory (Adv. Mater. 29/2012). Advanced Materials, 2012, 24, 3898-3898.	21.0	2
190	Effect of top electrodes on photovoltaic properties of polycrystalline BiFeO ₃ based thin film capacitors. Nanotechnology, 2011, 22, 195201.	2.6	136
191	Mechanism of nonvolatile resistive switching in graphene oxide thin films. Carbon, 2011, 49, 3796-3802.	10.3	141
192	Giant anisotropic magnetoresistance in bilayered La1.2Sr1.8Mn2O7 single crystals. Applied Physics Letters, 2011, 98, 212503.	3.3	18
193	Improvement of resistive switching in Cu/ZnO/Pt sandwiches by weakening the randomicity of the formation/rupture of Cu filaments. Nanotechnology, 2011, 22, 275204.	2.6	106
194	Microstructure dependence of leakage and resistive switching behaviours in Ce-doped BiFeO ₃ thin films. Journal Physics D: Applied Physics, 2011, 44, 415104.	2.8	53
195	Nonvolatile resistive switching memory based on amorphous carbon. Applied Physics Letters, 2010, 96,	3.3	133
196	Resistance switching in polycrystalline BiFeO3 thin films. Applied Physics Letters, 2010, 97, .	3.3	139
197	Nonvolatile resistive switching in metal/La-doped BiFeO ₃ /Pt sandwiches. Nanotechnology, 2010, 21, 425202.	2.6	104
198	Initial Adsorption of C60 Molecules on Si(111)-7*7 Surface with Al Nanocluster Array. E-Journal of Surface Science and Nanotechnology, 2010, 8, 354-357.	0.4	1

#	Article	IF	CITATIONS
199	Possible origins of the magnetoresistance gain in colossal magnetoresistive oxide La0.69Ca0.31MnO3: Structure fluctuation and pinning effect on magnetic domain walls. Applied Physics Letters, 2009, 95, 092504.	3.3	8
200	Magnetism, transport, and specific heat of electronically phase-separated Pr _{0.7} Pb _{0.3} MnO ₃ single crystals. Journal of Physics Condensed Matter, 2009, 21, 076002.	1.8	3
201	Nonvolatile resistive switching in graphene oxide thin films. Applied Physics Letters, 2009, 95, .	3.3	228
202	Anomalously large anisotropic magnetoresistance in a perovskite manganite. Proceedings of the National Academy of Sciences of the United States of America, 2009, 106, 14224-14229.	7.1	74
203	Thermal stability of Al nanocluster arrays on Si (111)-7 × 7 surfaces. Nanotechnology, 2006, 17, 2018-2022.	2.6	8
204	Current effects and topology of current paths in single crystalline Pr[sub 0.7]Pb[sub 0.3]MnO[sub 3]. Journal of Applied Physics, 2006, 100, 113902.	2.5	1
205	Nanopatterning of perovskite manganite thin films by atomic force microscope lithography. Nanotechnology, 2005, 16, 28-31.	2.6	24
206	Ordered Nano-Islands on (La,Ba)MnO ₃ Thin Film Surface by Self-Organization. Journal of Nanoscience and Nanotechnology, 2004, 4, 982-985.	0.9	1
207	Atomic force microscope lithography in perovskite manganite La0.8Ba0.2MnO3 films. Journal of Applied Physics, 2004, 95, 7091-7093.	2.5	22
208	Relaxation of nanopatterns on Nb-doped SrTiO3 surface. Applied Physics Letters, 2004, 84, 2670-2672.	3.3	15
209	Structure, magnetic properties and phase separation of Nd0.5Ca0.5Mn1â^'xGaxO3 (0x0.1). Journal of Magnetism and Magnetic Materials, 2003, 265, 248-256.	2.3	9
210	Magnetic transition and large low-field magnetoresistance near Curie temperature in polycrystalline La2/3A1/3MnO3 (A=Ca,Sr). Journal of Applied Physics, 2003, 93, 8092-8094.	2.5	10
211	Nanoscale observation of room-temperature ferromagnetism on ultrathin (La,Ba)MnO3 films. Applied Physics Letters, 2003, 83, 1184-1186.	3.3	31
212	Antiferro- to ferromagnetic transition and large magnetoresistance in YMn6Sn6â^'xTix (x=0–1.0) compounds. Journal of Applied Physics, 2002, 91, 5250-5253.	2.5	18
213	Large low-field magnetoresistance of phase-separated single-crystalline Pr0.7Pb0.3MnO3. Applied Physics Letters, 2002, 80, 3367-3369.	3.3	19
214	Phase separation induced by doping at Mn sites in Nd[sub 0.5]Ca[sub 0.5]Mn[sub 0.98]Ga[sub 0.02]O[sub 3]. Journal of Applied Physics, 2002, 91, 7941.	2.5	3
215	Direct observation of phase separation in La0.45Sr0.55MnO3â^1ŕ. Journal of Applied Physics, 2002, 92, 7404-7407.	2.5	8
216	Superparamagnetism and transport properties of ultrafine La2/3Ca1/3MnO3powders. Journal of Physics Condensed Matter, 2001, 13, 141-148.	1.8	45

#	Article	IF	CITATIONS
217	Low-temperature magnetization step and its training effects in phase-separated La0.5Ca0.5MnO3. Journal of Physics Condensed Matter, 2001, 13, 1973-1978.	1.8	10
218	Magnetocrystalline anisotropy of Y2(Fe1-xCox)15Ga2compounds. Journal Physics D: Applied Physics, 2000, 33, 1446-1449.	2.8	0
219	Lattice effects of doping the Mn sites in La0.5Ca0.5MnO3. Journal of Applied Physics, 2000, 88, 5924-5927.	2.5	5
220	Magnetoresistance of La0.5Sr0.5MnO3 nanoparticle compact. Journal of Applied Physics, 2000, 87, 5582-5584.	2.5	39
221	Effects of the relative proportion of ferromagnetic and charge-ordered phases on the metal–insulator transition temperature in La0.5Ca0.5Mn1â^'xGexO3. Journal of Applied Physics, 2000, 88, 7041-7044.	2.5	6
222	Magnetic and transport properties of Sn-doped La0.5Ca0.5MnO3. Journal Physics D: Applied Physics, 2000, 33, 1982-1984.	2.8	6
223	Magnetic properties and colossal magnetoresistance of the perovskites La2/3Ca1/3Mn1â^'xTixO3. Journal of Applied Physics, 2000, 87, 5597-5599.	2.5	38
224	Magnetic glass behavior and magnetoresistive properties of perovskite cobaltitesLa0.7Sr0.3Co1â^'yGayO3. Physical Review B, 1999, 60, 14541-14544.	3.2	10
225	Structure and magnetic properties of (x= 0-3) compounds with R = Y and Pr. Journal of Physics Condensed Matter, 1998, 10, 2445-2452.	1.8	13
226	Multifunctional Optoelectronic Device Based on Resistive Switching Effects. , 0, , .		4
227	Observation of Atomicâ€Order Engineered Martensitic Transformation in Ni 45 Co 5 Mn 37 In 13 Metamagnetic Shape Memory Alloys. Advanced Engineering Materials, 0, , 2100711.	3.5	Ο